UNIVERSITY OF CALIFORNIA SAN DIEGO

Sampling methodologies for analysis of particulate matter in gas emissions from volcanic eruptions

A Thesis submitted in partial satisfaction of the requirements
for the degree Master of Science

in

Earth Sciences

by

Katherine Bounassi

Committee in charge:

Professor Geoffrey Cook, Chair
Professor James Day
Professor Margo Odlum

2026

The Thesis of Katherine Bounassi is approved, and it is acceptable in quality and form for publication on microfilm and electronically.

University of California San Diego

2026

TABLE OF CONTENTS

LIST OF FIGURES

LIST OF TABLES

LIST OF ABBREVIATIONS

BSE	Backscatter electron
EDS	Energy Dispersive X-ray Spectroscopy
HVO	Hawai'i Volcano Observatory
ICP/MS	Inductively Coupled Plasma/Mass Spectrometry
MCE	Mixed Cellulose Ester
PM	Particulate Matter
PGE	Platinum-Group Elements
PC	Polycarbonate
PTFE	Polytetrafluoroethylene
SEM	Scanning Electron Microscope
UAS	Unoccupied Aircraft System
UAV	Unmanned Aerial Vehicle

ACKNOWLEDGEMENTS

Above all, I would like to thank Geoffrey Cook for his unwavering support and encouragement throughout this experience. Thank you for your contagious enthusiasm and joy for volcanoes and the opportunity to experience field work in Hawai'i. I will always be grateful for your guidance and instruction. To James Day, thank you for the support, expertise, and patience through each step. To Margo Odlum, thank you for being an amazing instructor, role model, and your passion for geology. I must also thank Heather Cook, you bring so much kindness and thoughtfulness to every situation that never goes unnoticed. I am immensely thankful for your willingness to participate and the time you have dedicated to helping me grow not just professionally but personally as well.

Additionally, I would like to thank Riley Meehan and the entire Scripps Makerspace staff for their passion for helping and engineering expertise. And to James Muller, thank you for your indispensable help with the SEM and your endless support. To Yash Srivastava, thank you for your time and willingness to help, whether it was answering questions or the SEM, you always showed an enthusiasm I am grateful for. To all my professors at Scripps Institution of Oceanography, you have all be instrumental in making me the geologist I am today. Thank you for the knowledge and experiences you have given me.

ABSTRACT OF THE THESIS

Sampling methodologies for analysis of particulate matter in gas emissions from volcanic eruptions

by

Katherine Bounassi

Master of Science in Earth Sciences

University of California San Diego, 2026

Professor Geoffrey Cook, Chair

The study of volcanic gas and associated particulate matter using filters and combination filter “packs” is a narrow field of research that can provide insight into geologic processes such as mantle geochemistry, magma sources, eruptive timing and dynamics, and potential human health impacts. This work offers a robust literature review paired with the development of

sampling methods for active volcanic plumes. Ground-based and unmanned aerial vehicle (UAV)-based sampling methods have been developed for efficient and safe sampling with the use of filters as a means of collection. Through a combination of geochemical, scanning electron microscope (SEM), and qualitative tests, it was determined that the Mixed Cellulose Ester (MCE) filter material is likely the most capable at particle collection and retention. UAV-based sampling is the preferred field sampling technique because it provides the best opportunity to get as close as possible to an eruption plume and the outgassing of aerosols and particles.

1. INTRODUCTION

Effusive basaltic eruptions, such as those in Hawai'i and Iceland, provide a relatively accessible and safe working environment for volcanic gas plume sampling near active vents. Geochemical analysis of aerosols and particulates (including metals) in a plume may provide insights on a wide range of topics, including mantle petrology (Crocket and Paul, 2004), magma sources (Mason et al., 2021), petrologic processes (Crocket and Paul, 2004), eruptive timing and dynamics (Mason et al., 2021), in addition to atmospheric chemistry (Ilyinskaya et al., 2021) and potential human health impacts (Ilyinskaya et al., 2021; Mandon et al., 2019). Currently, there are no well-documented or established methods for sampling volcanic gas plumes. Most studies up until this point have used a variety of methods to collect aerosols and particulates, and they have employed "filter packs" utilizing a variety of materials to trap samples for later analysis (Ilyinskaya et al., 2017; Ilyinskaya et al., 2021; Mason et al., 2021). These filters have largely been repurposed from the environmental safety and air quality industry and are employed using practices for air quality sampling and analysis.

Unmanned aerial vehicles (UAV or "drones") are a relatively new technology, and one that holds great promise in volcano gas sampling. Previously, gas sample collection and field work near active volcanos was dangerous due to hazards like ejecta and gas emissions. With the use of a UAV, much of this risk is eliminated as control of the device may be done at a safe distance. Preliminary work (unpublished, by this research group) using UAVs in Iceland (Svartsengi volcanic system, 2024) collected particulate samples using Mixed Cellulose Ester (MCE) filters. Sampling yielded valid geochemical data indicating that future studies are warranted. Based on the experiences of this sampling and analysis, it was determined that more robust methods and practices would be useful to future research.

This work provides a unique perspective on both ground and air sampling techniques that may be conducted for particulate matter (PM) collection using filters. With the use of a UAV, sampling from directly within a plume is a future possibility; although, conducting ground and airborne collection simultaneously for comparison would be the ideal scenario. This research developed and assessed the efficacy of sampling methods for active volcanic plumes, including ground-based and UAV-based methods. Additionally, a comprehensive literature review was undertaken to provide both a stand-alone summary of methods to this date, and to inform method development. Methods development includes assessment of filter material, pore size, location of sampling apparatus on the UAV, and sampling duration in addition to analysis procedures. The use of UAV and ground sampling with a filter-pump apparatus demonstrates the validity that sampling a volcanic plume during an eruption has the potential to yield valuable results regarding mantle composition, magma source, PM present, etc.

Two locations were identified as potential sampling sites: Hawai'i (Kilauea volcano seen in Figure 1); and Iceland, on the Reykjanes Peninsula. Both volcanic systems have recently been host to relatively frequent basaltic eruptions with good opportunities to conduct sampling. Iceland, specifically, is ideal as vent-proximal UAV and ground sampling is possible with the ongoing series of eruptions at Svartsengi/Sundhnúkur crater row. Sampling at Kilauea is restricted to ground sampling just outside the boundary of Hawai'i Volcanoes National Park at greater distances (>7 km) due to restrictions enacted by the U.S. National Park Service. Unfortunately, during this research Iceland did not erupt and consequently UAV methods were not tested. However, since December 2024, the Halema'uma'u crater at Kilauea volcano on Hawai'i Island, Hawai'i has been highly active, alternating between lava fountaining events (47 episodes at the time of writing, May 2026) and periods of repose. The fountaining events provide

a reasonable opportunity for ground sampling of gases and particulates. Eruptions have occurred anywhere from every few days, to multiple weeks apart with eruption durations between 2 hours to over 10 hours. Lava fountaining events have the capability to produce fountains over 500 meters in height with the gas plume reaching significant altitudes (over 6000 meters). Between active fountaining events there is regular, ongoing degassing that increases leading up to an eruption along with potential short bursts of lava from the two active vents.

For this study, ground-based sampling was conducted during the 36th fountaining episode on November 9th, 2025 (Figure 1). The eruptive episode began at 11:15 a.m. Hawaiian Standard Time and activity ceased roughly 5 hours later at 4:16 p.m. according to the Hawai'i Volcano Observatory (HVO). The main north and south vents were actively fountaining in addition to a smaller southern vent (Figure 1). HVO reported the approximate volume of lava erupted to be 8.1 million cubic meters and the approximate maximum fountain height to be 386 meters. Sampling was conducted at a location on the boundary of Hawaii Volcanoes National Park, approximately 7 kilometers to the west of the active vent, and downwind (Figure 2). Several filters were analyzed and inspected using Scanning Electron Microscopy (SEM) to assess efficacy of particle collection. Additionally multiple filters were analyzed for geochemistry, specifically to determine if metals and platinum group elements (PGE's) were collected by the various types of filters deployed.

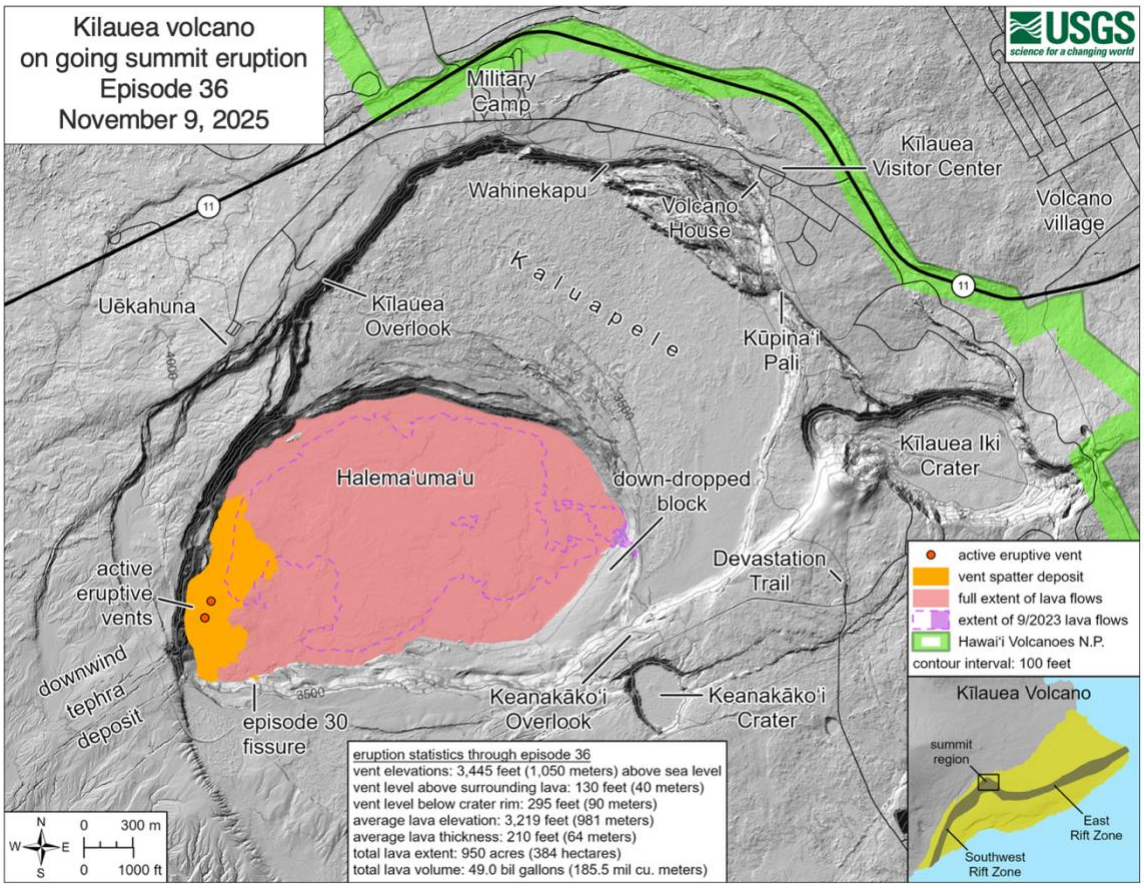

Figure 1: Map of Halemaʻumaʻu crater at Kilauea volcano on Hawai'i Island with data for the eruption on November 9, 2025 (modified from Hawaiian Volcano Observatory, 2025).

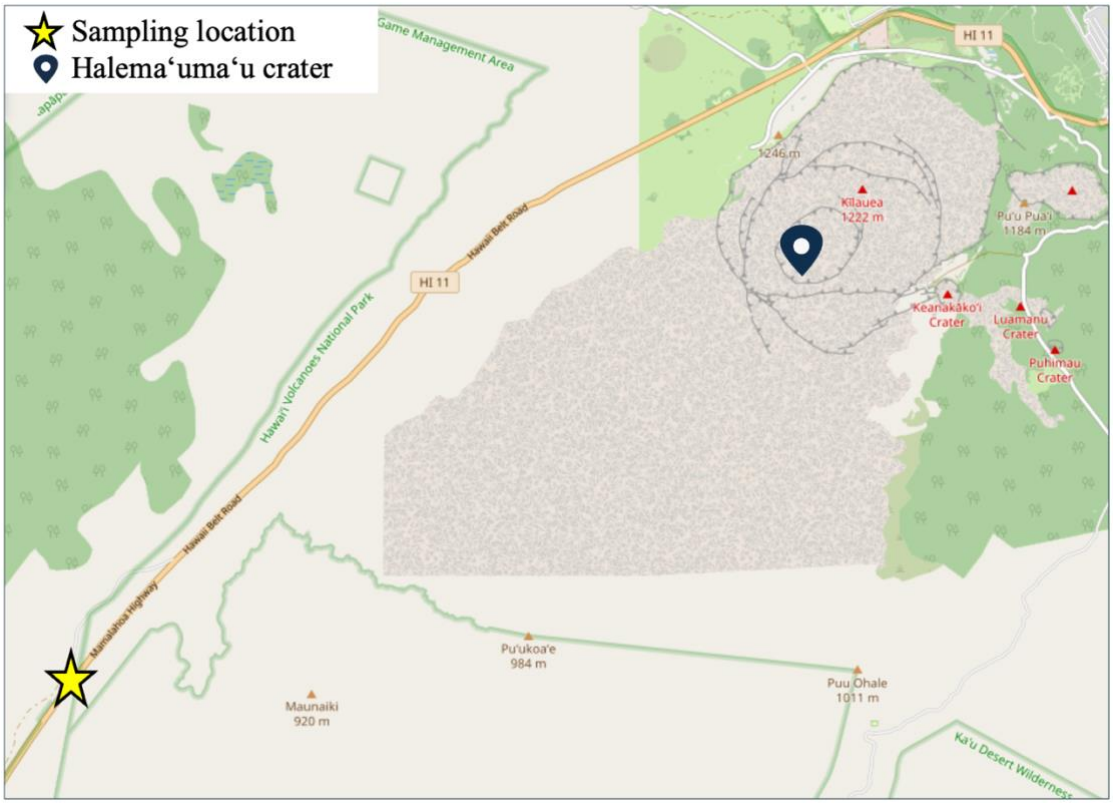

Figure 2: Map depicting Halema‘uma‘u crater at Kilauea volcano on Hawai’i Island with sampling location denoted (modified from Hawaiian Volcano Observatory, 2025).

2. LITERATURE REVIEW

The composition of volcanic gas plumes is of interest for a variety of volcanological and geochemical reasons. Gas composition and particle content may reflect petrologic processes such as magma fractionation (Mather et al., 2008; Mason et al., 2021) and partial melting (Crocket and Paul, 2004) in addition to provide insight into metal pollutants (Ilyinskaya et al., 2021) and human health impacts (Mandon et al., 2019) of eruptions. Most commonly, basaltic (passive) volcanoes have been studied due to their relatively low-risk level and the ability to get within close range of the vent either with sampling tools or as an individual. A range of techniques have been developed for plume sampling. Filter packs, a combination of different filter materials to collect gases and PM, are a low-cost and accessible option that is often used and common in industry for environmental safety and air quality tests. A robust review was conducted of the current literature in industry and research revolving around filter packs and volcanic plume sampling, which found that the development of filter packs in the study of volcanic gas and particulate matter (PM) dates to the 1970s (Naughton et al., 1975) and has since undergone improvements and changes. Sampling requires only the volcanic plume, ambient air, or other gaseous forms near the active volcanic vent; it does not include lava or rock samples, although these may be used in comparison or to further the PM and gas analysis results (Menard et al., 2014). Of note, a multitude of approaches have been suggested and tested without a specific, robust, standardized method. Instead, a commonality in methods is understood and observed throughout prior research. As a result, limitations and variations in technique exist whilst attempting to research and analyze volcanic gas and PM. There is no apparent set procedure for filter pore size, sampling location (ground-based or airborne), sampling duration, storage method

(in a cold environment or not), and perhaps most importantly which filter material is most effective such as MCE, Polytetrafluoroethylene (PTFE), etc.

The most commonly used sampling method involves a filter pack consisting of a particulate filter followed by two to four impregnated gas filters (Aiuppa et al., 2002; Aiuppa et al., 2004; Allen et al., 2000; Crowe et al., 1987; Finnegan et al., 1989; Ilyinskaya et al., 2017; Ilyinskaya et al., 2021; Mandon et al., 2019; Martin et al., 2008; Mason et al., 2021; Mather et al., 2012; Mather et al., 2008; Mather et al., 2003; Menard et al., 2014; Moune et al., 2010; Olmez et al., 1986; Pfeffer et al., 2013; Shinohara and Witter, 2005; Stefánsson et al., 2017). Similar methods were used by Hinkley (1991), Naughton et al. (1975), and Wittmer et al. (2014) in which a bubbler was used in addition to a filter. The combination of particulate and gas filters facilitates the concurrent collection of PM and gases. In nearly all the uses of the filter pack, a pump was used to facilitate and sometimes quantify air flow. However, flow rate was not necessarily recorded and/or checked regularly to ensure consistency. Additionally, uncertainty may be introduced depending on when the pump is turned on. For example, the pump may be turned on either when in the plume or simply nearby. Starting the pump while samples are directly in the plume helps to ensure the filters are most representative of the plume only rather than ambient air (Mandon et al., 2019). A remotely operated switch may need to be used to accomplish this. In terms of filters used for sampling, a variety exists including MCE, PTFE, polycarbonate (PC) membrane, and Whatman®. PTFE and Whatman® filters are the most used in previous studies. It has been shown that PTFE filters are capable and highly efficient at collecting particles of all sizes with a single filter layer (Allen et al., 2000). Pore size used varied between studies such as: 0.8µm (Ilyinskaya et al., 2021), 1 µm (Mandon et al., 2019; Stefánsson et al., 2017), and 12-µm (Allen et al., 2000) with a whole filter diameter of 47 mm being

common. In other studies, diameter and pore size were not specified or described. Gas filters are typically Whatman® quantitative filter papers (Ilyinskaya et al., 2021; Mason et al., 2021) and alkali-impregnated materials that are located further down the pack, following the PM filters. The purpose of base-treating the filters is to facilitate the capture of acidic gases (Ilyinskaya et al., 2021). The solution used to impregnate the gas filters generally differs between studies, however an alkali solution is always used. Examples of types of solutions used include: 0.1 M Na_2CO_3 + 2% glycerol (Allen et al., 2000), 5% K_2CO_3 + 1% glycerol (Mason et al., 2021), 10% $NaHCO_3$ and 10% glycerol in 1:1 methanol/distilled deionized water (Martin et al., 2008). Multiple gas filters are necessary due to the filter first in the series potentially becoming fully saturated (Ilyinskaya et al., 2021), thus a subsequent filter(s) ensures continued gas capture and breakthrough detection. As a result, it is important to note that in some cases gas concentrations may not be best suited for calculating gas to PM ratios as they may represent a minimum value (Ilyinskaya et al., 2021). Finally, blanks were commonly used (Allen et al., 2000; Crowe et al., 1987; Finnegan et al., 1989; Ilyinskaya et al., 2021; Mandon et al., 2019; Martine et al., 2008; Mather et al., 2003; Mather et al., 2008; Mather et al., 2012; Menard et al., 2014; Moune et al., 2010; Naughton et al., 1975; Olmez et al., 1986; Pfeffer et al., 2013; Stefánsson et al., 2017; Wittmer et al., 2014) for corrections and potentially quantifying contamination.

Sample collection varied in terms of location/distance to the plume, ground or aerial, and duration in the plume. Sampling was commonly conducted in a variety of ways: on the ground at a vent-proximal location (such as a crater rim) downwind of the plume (Mather et al., 2012; Martin et al., 2008; Menard et al., 2014); within the plume above ground via aircraft (Pfeffer et al., 2013) or using an Unmanned Aircraft System (UAS)/Unmanned Aerial Vehicle (UAV) (Ilyinskaya et al., 2021; Mason et al., 2021; Mandon et al., 2019); or on the ground at set

distances away from the plume (Allen et al., 2000; Ilyinskaya et al., 2021). For the most ideal sampling location, the goal of the study needs to be considered. Near ground sampling and aerial sampling is typically used for trace metal emission directly at the source. Sampling further from the source is more suited for research regarding changes in the plume over time and distance (Ilyinskaya et al., 2021) as well as human health impacts (Allen at al., 2000). Additionally, when using a UAS/UAV the placement of the sampling tools is necessary to consider due to rotor wash and the flow field as this may have a non-negligible influence on particle distribution (Hedworth et al., 2021). Despite the flow field not influencing particle size segregation overall particle distribution may be impacted (Hedworth et al., 2021). Consequently, placing the sampling tools above the drone is best-practice and provided results closest to that of a drone-free environment (Tran, 2019; Hedworth et al., 2021), although some studies have suggested that a non-turbulent dead zone is located on the underside instead (Tipayarom et al., 2024). Next, the duration of the sampling is an important variable that is usually considered with the sampling location in mind. When attempting to sample at an eruption site changes in atmospheric variables may make sampling difficult (Stefánsson et al., 2017), thus leading to shorter durations. In addition, battery life of a UAV (and flight distance to sampling location) may inhibit sampling duration to as little as 5 minutes (Mandon et al., 2019). Without limitations such as the ones mentioned, sampling can last anywhere between 20 minutes (Mandon et al., 2019) to multiple days using campaign-style ground monitoring (Ilyinskaya et al., 2017). Saturation of filters, as mentioned earlier, is additionally considered when selecting a sampling duration.

After samples have been collected, storage and transportation methods are important considerations. Samples are preferably unaltered for analysis, though methods for accomplishing this were shown to differ. For instance, in one study (Mather et al., 2008) exposed filters were

sealed in plastic bags and subsequently stored in a freezer when able. The purpose of this is to decrease the risk of further reactions occurring (Mather et al., 2008). Another method consisted of transferring the filters with metal-free tweezers and gloves to polypropylene bags (Mason et al., 2021); or, closed with a plastic lid and later placed in polypropylene bags once indoors (Ilyinskaya et al., 2017). Some samples were stored in a cold place, like a refrigerator or freezer, until analysis (Crowe et al., 1987; Martin et al., 2008; Mather et al., 2008; Mather et al., 2003). In most other studies storage methods were not clarified.

Analysis greatly differed in terms of methods and equipment used. Depending on the purpose and goals of a study, analytical methods are variable and therefore are not necessarily a vital component while attempting to formalize filter pack methods. An example of a common analytical method includes inductively coupled plasma-mass spectrometry (ICP-MS) to quantify elements of interest (Allen et al., 2000; Ilyinskaya et al., 2017; Ilyinskaya et al., 2021; Mandon et al., 2019; Mason et al., 2021; Mason et al., 2022; Mather et al., 2012; Menard et al., 2014; Moune et al., 2012; Wittmer et al., 2014). Extracts are typically obtained from the filters and then analyzed using ICP-MS. In obtaining these extracts, liquid solutions are combined with the filters. These solutions varied between studies and are devised to aid in accomplishing the individual preferred analysis.

The filter material plays an important role in the solutions components. For instance, PTFE filters may have an extracting solution composed of Milli-Q (MQ) water and propan-2-ol to reduce the hydrophobicity of the PTFE filters (Ilyinskaya et al., 2021; Mason et al., 2021). A cascade impactor and a pump were occasionally used during sampling simultaneously with the filters (Hinkley, 1991; Ilyinskaya et al., 2017; Ilyinskaya et al., 2021; Mason et al., 2021; Mather et al., 2012;). The impactor is able to separate particles by size, while particle filters simply

collect everything with undifferentiated size. Through the comparison of results, it is possible to determine the amount of each metal that falls into a certain size category as a fraction of the total metal amount collected on the particle filter (Hinkley, 1991).

Interpretation of results is additionally variable depending on the purpose and focus of the research, however key elements are still necessary to discuss such as method of quantification for trace elements and/or aerosol compositions. Quantification is highly dependent on sampling method and level of accuracy. For instance, trace element fluxes are estimated based on the measured X/SO_2 ratio as the fluxes cannot be measured directly (Mason et al., 2021). SO_2 emission rate was independently measured (Mason et al., 2021). However, in another case, due to the saturation levels the samples are recommended to be representative of minimum values and thus not used to calculate the gas-to-PM ratios (Ilyinskaya et al., 2021). Further, it is possible to have the acid gases and aerosol compositions being a fraction of the total material collected in a filter pack in $\mu g.g^{-1}$ (or parts per million) (Mandon et al., 2019).

Reflecting on this literature, there are clear gaps in standardization at all stages of research. Some such standardizations are less important than others, especially when considering the goals of a study. Sampling duration is one such standard. As mentioned before, sampling conducted very close to the plume/crater typically has a shorter duration than more distal sampling because of natural consequences and/or equipment limitations, such as battery life (Mandon et al., 2019). Arguably the more important methods in need of standardization include filter material (including pore size), ground vs aerial sampling, and pump use. Through the creation of a formal, practical, and adaptable method, a better understanding of volcanic plumes and their PM components will be accomplished.

3. METHODS

3.1 Field (ground) sampling procedure

Prior to arriving at the sampling location, sealable plastic bags were labeled with the location, number, filter type (MCE, PC, etc.) and filter pore size. Two SKC AirLite® Sample Pumps were calibrated to 1 L/min and connected with a splitter to allow for two sample filters to be attached per pump. Calibrations were done respectively to account for any variation in splitters. The pumps were secured to a tripod, ensuring that there were no kinks in the tubing when attaching to filters to the pumps (Figure 3).

On November 9th, 2025, episode 36 of the ongoing Kilauea eruption began at 11:15 a.m. Hawaiian Standard Time. At roughly 1:00 p.m. the ground sampling tripod apparatus was set up approximately 7 km downwind of the vent (Figure 3). GPS Coordinates were recorded at the location of the tripod. Two of each MCE 0.45µm, MCE 0.8µm, PTFE 1.0µm, and PC 0.8µm filters were removed from their respective bags and attached to the tripod facing head to wind and in the direction of the vent. 4 filters, one of each type, was sampled using the pump. The other 4 filters were sampled open-faced, meaning the cartridge face was removed and no pump was used. 2 15-minute periods were chosen back-to-back leading to a total of 16 filters collected. After each duration, the pump was turned off, and the filters were disconnected and each filter placed in the appropriate prelabeled bags. Blanks for each filter type and pore size used were placed in prelabeled bags at the sampling site as well.

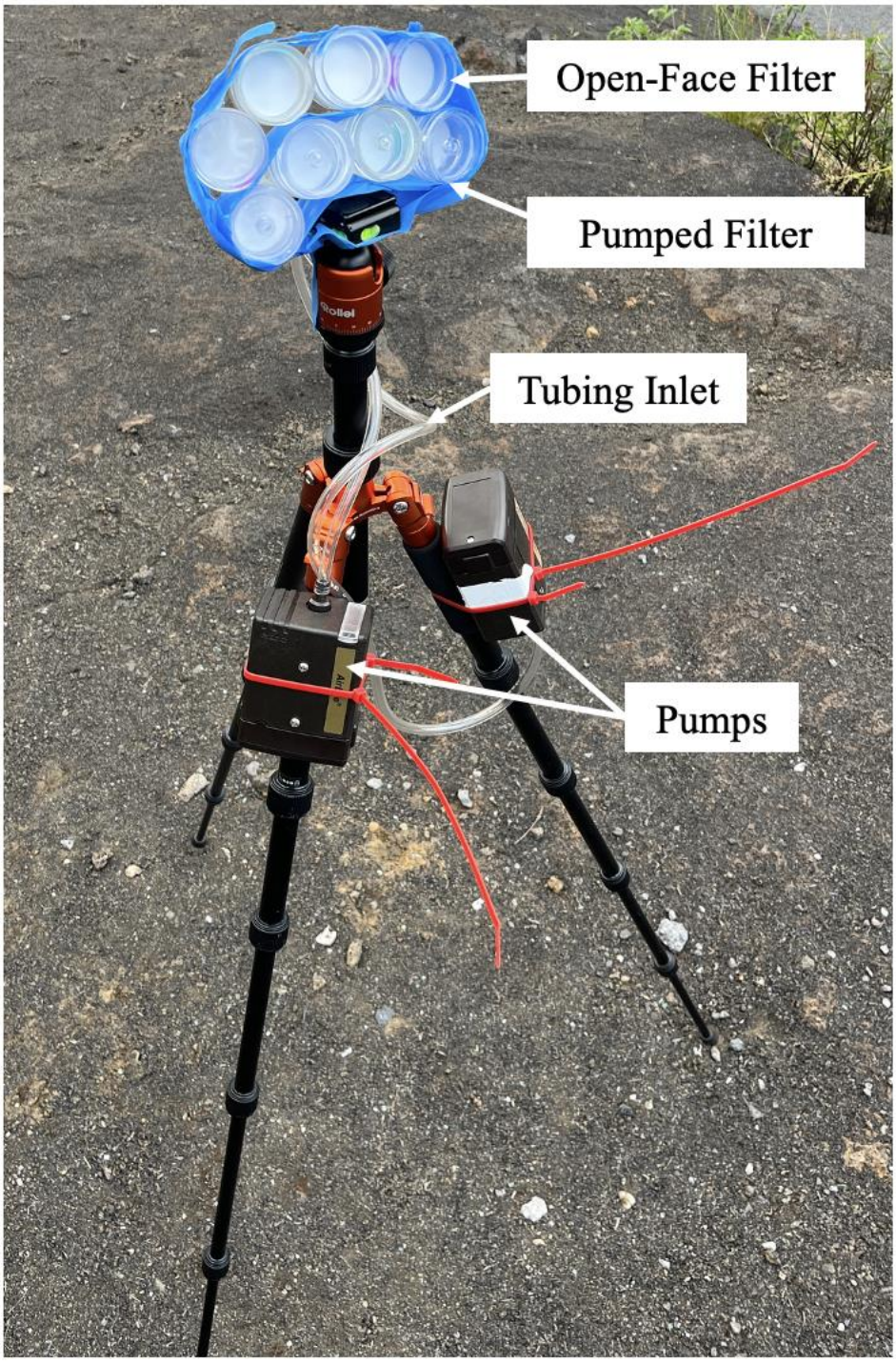

Figure 3: Labeled ground sampling apparatus used during the sampling of 36th Kilauea eruptive episode. Components include two pumps, tubing inlets, filters attached to a pump, and filters that are sampling open-face without a pump.

3.2 Filter evaluation and analysis

To evaluate the nature of filter materials and their ability to collect particulates, backscatter electron (BSE) images of blank MCE 0.45µm, MCE 0.8µm, PTFE 1.0µm, and PC 0.8µm filters were obtained using a Nanoscience Instruments Phenom XL variable-pressure desktop SEM at Scripps Institution of Oceanography, UC San Diego. The filters were loaded and affixed to the SEM stage with conductive carbon tape, and the instrument was pumped down to a low vacuum state (60 Pa) to reduce the risk of sample charging. Analyses utilized a 10 kV accelerating voltage and "image" intensity to balance brightness, resolution, and beam damage to the filters. The electron beam was focused on each filter at a 2x higher magnification before demagnifying to the final image's field of view. All filters were imaged at 10,000x magnification, except PTFE (5,000x due to beam-induced damage at greater magnification). BSE image acquisition settings comprised "best" quality (i.e., slowest scan speed), 2048-pixel resolution, and TIFF (lossless) file format. Brightness and contrast were adjusted manually for each filter to achieve visually similar image-average grayscales.

To evaluate whether field-exposed filter cassettes captured any volcanic particulates, a BSE image of two MCE 0.45µm filters (one open-faced and one pumped) field sampled in Hawai'i were imaged via SEM-BSE, as seen in Figures 4 and 5, using the same instrument and data acquisition parameters as the blanks. Images were taken in the center and in roughly four quadrants (i.e. top, bottom, sides) for each filter. Following this procedure, larger particles were imaged when found.

Additionally, MCE 0.45µm filters were tested in the lab for "capture efficacy" using a controlled experiment in which a blank filter was manually contaminated without a pump using ash-sized tephra collected from the 36th eruption period at Kilauea, and fine ash from the 1980

eruption of Mt. St. Helens. One half was the tephra, and the other half was the ash. Larger particles (over 5µm in length) to smaller particles (less than 3µm) were seen for both the tephra and the ash. Notably, however, larger particles were susceptible to electron beam damage. For a direct comparison between filters, blanks of each were SEM-BSE imaged.

Lastly, MCE 0.8µm and PTFE 1.0µm filters were artificially contaminated in a separate lab-based test using powdered tephra (sieved to <75µm, from the Groundhog scoria cone in Golden Trout, California) with the goal of better understanding the level of PM adhesion to the different filter materials. The tephra was placed in the tubing that was attached to the front of the filters. The back of each filter was attached to a pump, via tubing, running at 1 L/min. Each filter collected tephra for 5 minutes to simulate sampling.

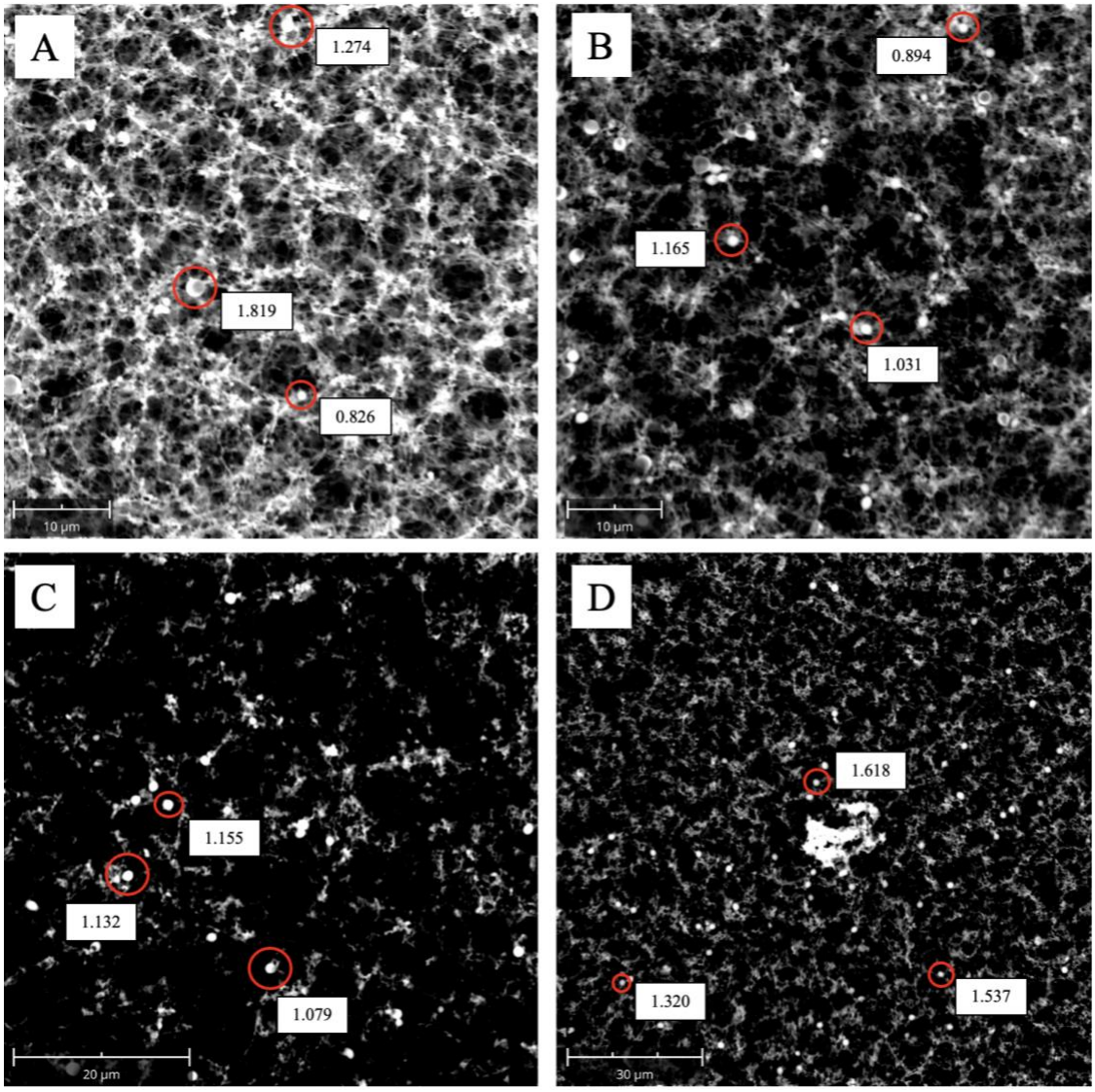

Figure 4: SEM-BSE imaging of MCE 0.45µm filter (field-sampled, Kilauea, Hawai'i with pump-based technique). SEM-BSE imaging, PM measured in µm and circled in red for reference. (A) and (B) 10µm scale, (C) 20µm scale, (D) 30µm scale.

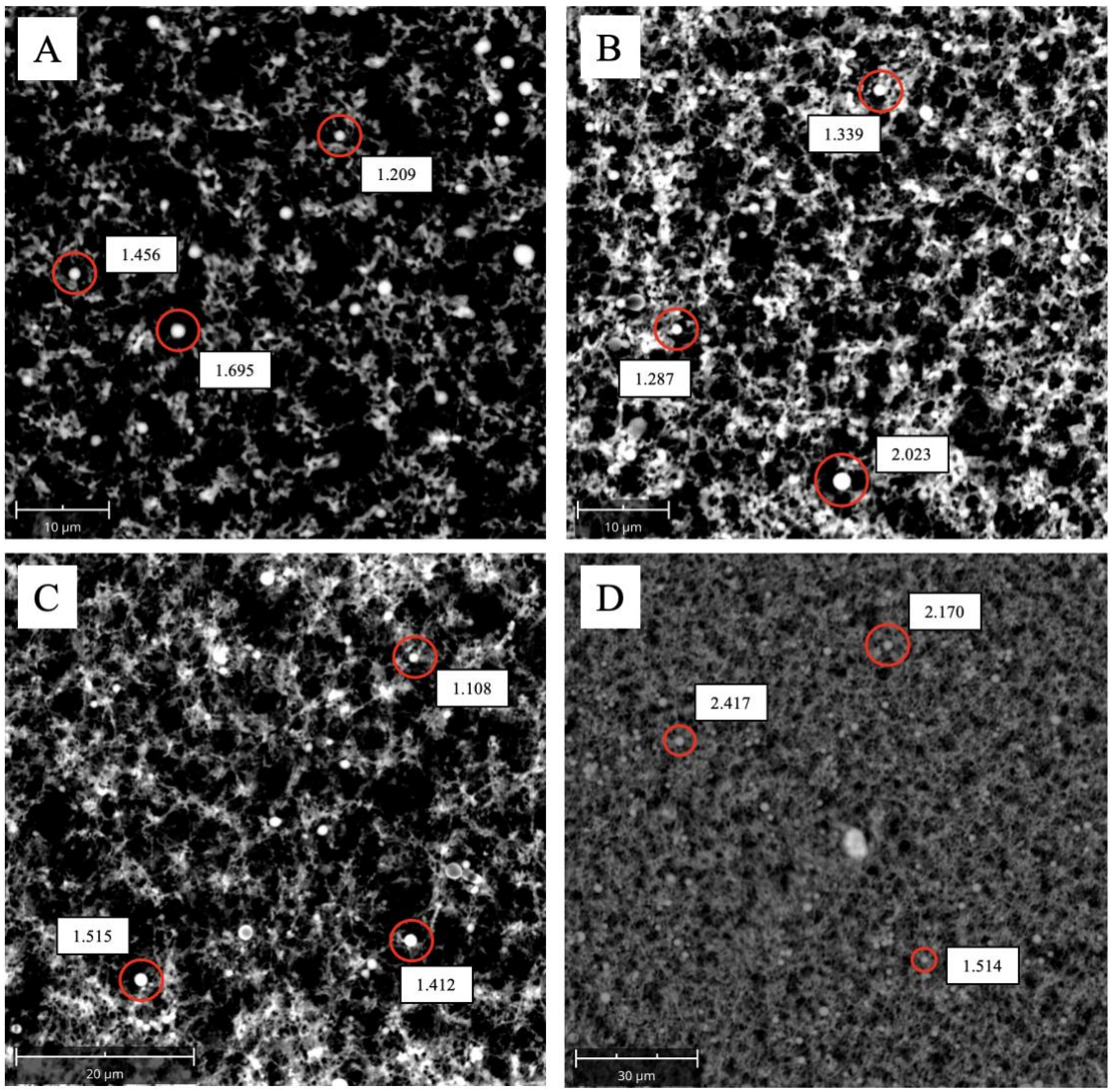

Figure 5: SEM-BSE imaging of MCE 0.45µm filter (field-sampled, Kilauea, Hawai'i with open-faced technique). SEM-BSE imaging, PM measured in µm and circled in red for reference. (A) and (B) 10µm scale, (C) 20µm scale, (D) 30µm scale.

3.3 Geochemical analysis

Both blank and field-sampled filters were analyzed for trace elements using the same techniques. 14 filters (2 MCE 0.45 filters having been reserved for SEM analysis) field sampled in Hawai'i during episode 36 were prepared and analyzed following methods at the *Scripps Isotope Geochemistry Laboratory (SIGL)*, Scripps Institution of Oceanography. Filters were first weighed then leached and/or dissolved in a 1 part 15.7 M HNO_3 to 4 parts 37M HF mixture on a hotplate at 110°C for 5 days. After drying down and multiple treatment with HNO_3 to remove fluorides, the samples were taken up in a 2% HNO_3 solution with a known quantity of a multi-element platinum group element spike (PGE: ^{99}Ru, ^{106}Pd, ^{185}Re, ^{191}Ir, ^{194}Pt) and indium to monitor instrument sensitivity and drift. Trace elements and PGE abundances were determined by being introduced into a *ThermoScientific* iCAP Qc quadrupole inductively coupled plasma mass spectrometer (ICP-MS) using a cyclonic spray chamber. All data are blank-corrected, with non-PGE trace element abundances determined by comparison of intensities with 0.1, 1 and 10 ng multielement calibration solutions. Isotope dilution was used to determine PGE abundances following methods outlined in Day et al. (2016).

3.4 Development of UAV (Aerial) sampling techniques

Aerial sampling provides a safe and efficient way to collect vent-proximal samples; however, challenges exist regarding the attachment of the sampling equipment to a UAV without hindering flying capabilities. If any motion sensors are covered or the payload exceeds capacity, the flying is greatly affected. Downdraft from the rotors may additionally alter collection,

especially if the filters are too close to the body of the UAV. An important consideration is that any protruding weight will alter the center of gravity and lead to the UAV being unstable.

The Makerspace, located at the Hydraulics Lab at Scripps Institution of Oceanography, UC San Diego was contacted to provide engineering expertise. Previous sampling efforts in Iceland (Cook, Day) were primitive, using zip ties and duct tape to attach filters to a UAV. Although those efforts were successful in collecting data, it was obvious that a more robust UAV sample setup was needed. The result is an improved prototype harness for the drone to attach a pump and a mast to hold multiple filters. Hedworth et al. (2021) determined that for the least amount of flow field interference from the drone propellers, the most suitable location for the filters would be on top of the drone. This is in part because there is less airflow interference above the propellers, but also specific to the drone used in our research; when one or more of the sensors on the drone are blocked safe flight becomes difficult, if not impossible. Initially, a pump was simply strapped onto the drone using zip ties and flown near the building to test the concept for the harness/pump location. A viable location for the pump was then determined and is unique to the drone model (Autel EVO II Dual 640T V3). If an alternate drone were to be used, it is recommended that time be taken to determine the safest location for a payload to be when flying.

A 3D model of the harness that allows for the pump to be secured was developed by Riley Meehan, Director of the Scripps Makerspace (Figure 6 and Figure 7). The program Autodesk Fusion 360 was utilized for all 3D designs. Multiple methods of holding the pump in place as well as potential designs for the filters to be secured were discussed. This involved adding a small, rounded cutout to the top of the harness to allow the pump to be screwed in using two screw holes on the pump as well as extending the harness to allow the pump to be fully

encased by the harness. The SKC Airlite pump has small bulges on either side. To accommodate this, channels were added to either side. These follow the entire length of the harness to allow the pump to fully slide in and out. Next, the filter holder was designed with the capacity to hold two filters and be secured to a mast via a hole on the bottom (Figure 6 and Figure 7). The final addition to the harness was an extension from the top that was extruded to allow for a mast to be secured. As a result, the harness could be attached to the filter holder using a mast with each the extension on the harness and hole on the filter holder being a tight fit.

Initial flight testing showed a maximum mast length of 135 mm being possible. Longer masts resulted in wobble and shaking of the drone compromising fight. A shortened mast would place the filters closer to the propellers and thus potentially be affected by rotor wash. As our study seeks to collect airborne particulates, not measure wind speed, it was concluded that a larger filter-propeller distance is primarily for turbulence measurements rather than aerosols. Further, due to the inlet used, biasing the number and size distribution of PM can be avoided. Therefore, a shortened mast with a height of roughly 77 mm is acceptable and sufficient for sampling. A total of three harnesses and filter holders were made. This is to allow two for field work with an additional one as a spare in the case of issues while sampling.

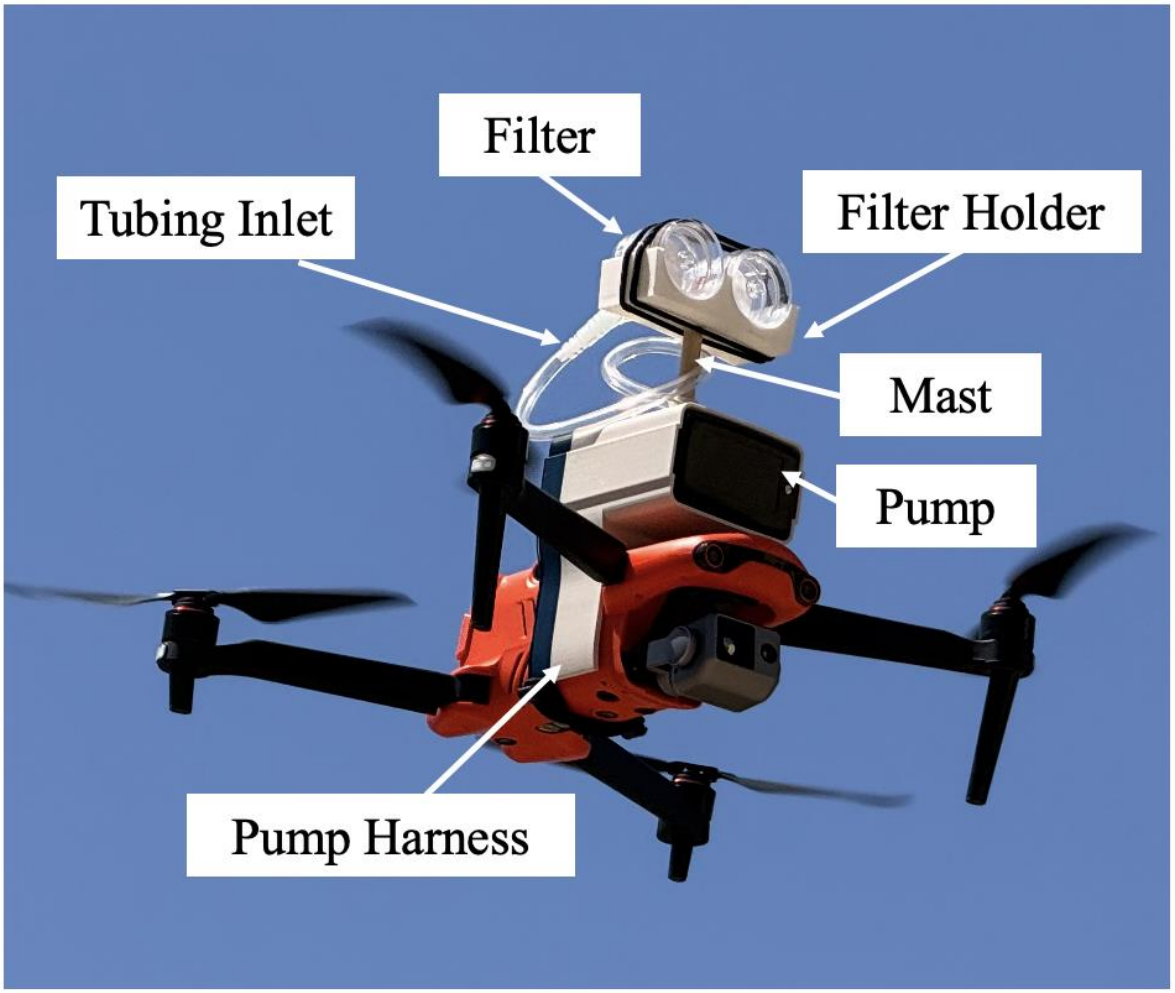

Figure 6: Labeled aerial sampling apparatus. Components include one pump secured in a pump harness, a tubing inlet, two filters secured in a filter holder, and a mast connecting the pump harness to the filter holder.

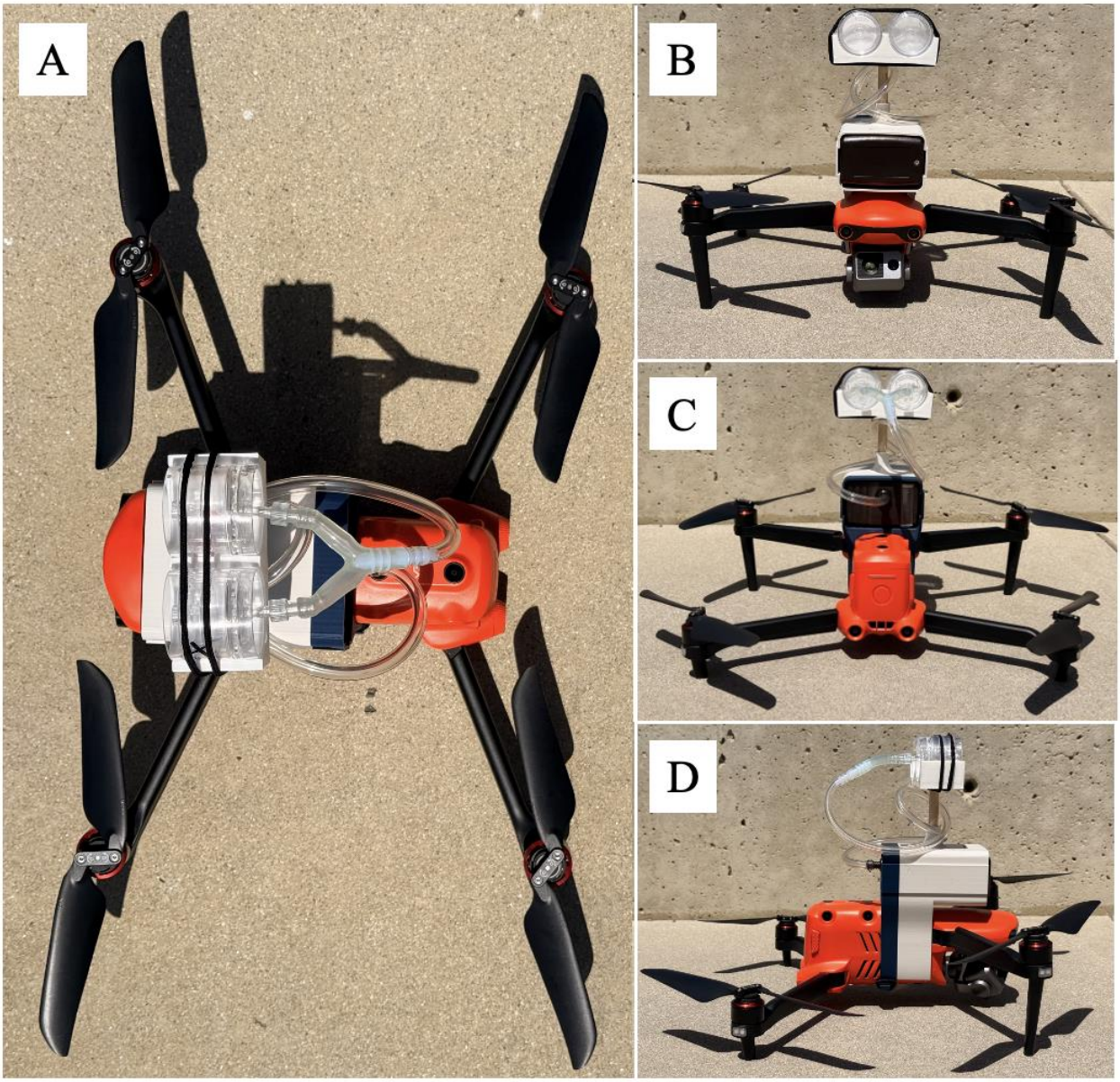

Figure 7: Aerial sampling apparatus. (A) top, (B) front, (C) back, (D) side.

3.5 Proposed aerial sampling procedure

Prior to arriving at the sampling location, plastic sealable bags are labeled with the location, number, material (MCE, PC, etc.) and pore size when necessary. Both pumps will be calibrated to an airflow of 1 L/min. Each pump will be connected to tubing with a splitter to allow for two filters to be attached. Calibrations were carried out in the field to account for the

splitter and potential pump differences. One pump remained as a spare, as the drone cannot carry a second pump with its payload weight limit (approximately 1 kg.).

For aerial sampling a maximum of two filters may fly at the same time. Filter pairs flown included a MCE 0.8µm and a PTFE 1.0µm. The purpose of this is to have at least one filter per sampling session for SEM, an MCE 0.8µm, with the remaining filters for geochemical analysis, both MCE 0.8µm and PTFE 1.0µm. Each pair of filters will sample the plume for ideally 20 minutes. Depending on conditions, the flight time may be reduced to accommodate. If there is remaining time the sequence will be repeated.

At the sampling location, the harness is secured to the filter holder via the mast. The harness is attached to the drone using three elastic ties ensuring the sensors are not covered. Filters are subsequently attached to the filter holder. The opened side of the filters will be pointing forward and parallel with respect to the drone. The back of the filter pack will have tubing secured to connected to the pump. The pump and accompanying timer are started when sampling is ready to begin. Following the sampling duration and the drone has returned, the pump is turned off and the tubing removed from the filters. Filters are placed in pre-labeled plastic bags for further protection from contamination and ease of transport. Blanks for each filter type and pore size used are additionally placed in their respective bags at the sampling site as well. A rock at the sampling site is ideally collected for geochemical analysis.

4. RESULTS

4.1 Blank filter analysis

SEM-BSE images of blank MCE 0.45µm, MCE 0.8µm, PTFE 1.0µm, and PC 0.8µm filters were taken to provide a visual reference of each filter and highlight the extent of differences in material composing the filters (Figure 8). The blank MCE 0.45µm and MCE 0.8µm filters are very similar with the sole difference being that the MCE 0.8µm had more open spaces in between the filter fibers as expected due to the larger pore size. Depth of the filter was identified by using darker areas corresponding to greater depth in the filter. Some bright, small, round areas were noted especially where the fibers connected. The PTFE 1.0µm filter was instantaneously affected by the electron beam on the SEM. Alteration was observed immediately in addition to a perceived movement of the filter making images difficult to acquire. The filter generally appears splotchy, with a mix of bright, white splotches with grey and black splotches. Lastly, the PC 0.8µm filter appears to be unaffected by the electron beam of the SEM. The resulting image was a light gray, flat surface with what would appear to be cut out circular holes that are interpreted to be the pores, as these are measured to be roughly 0.8 µm.

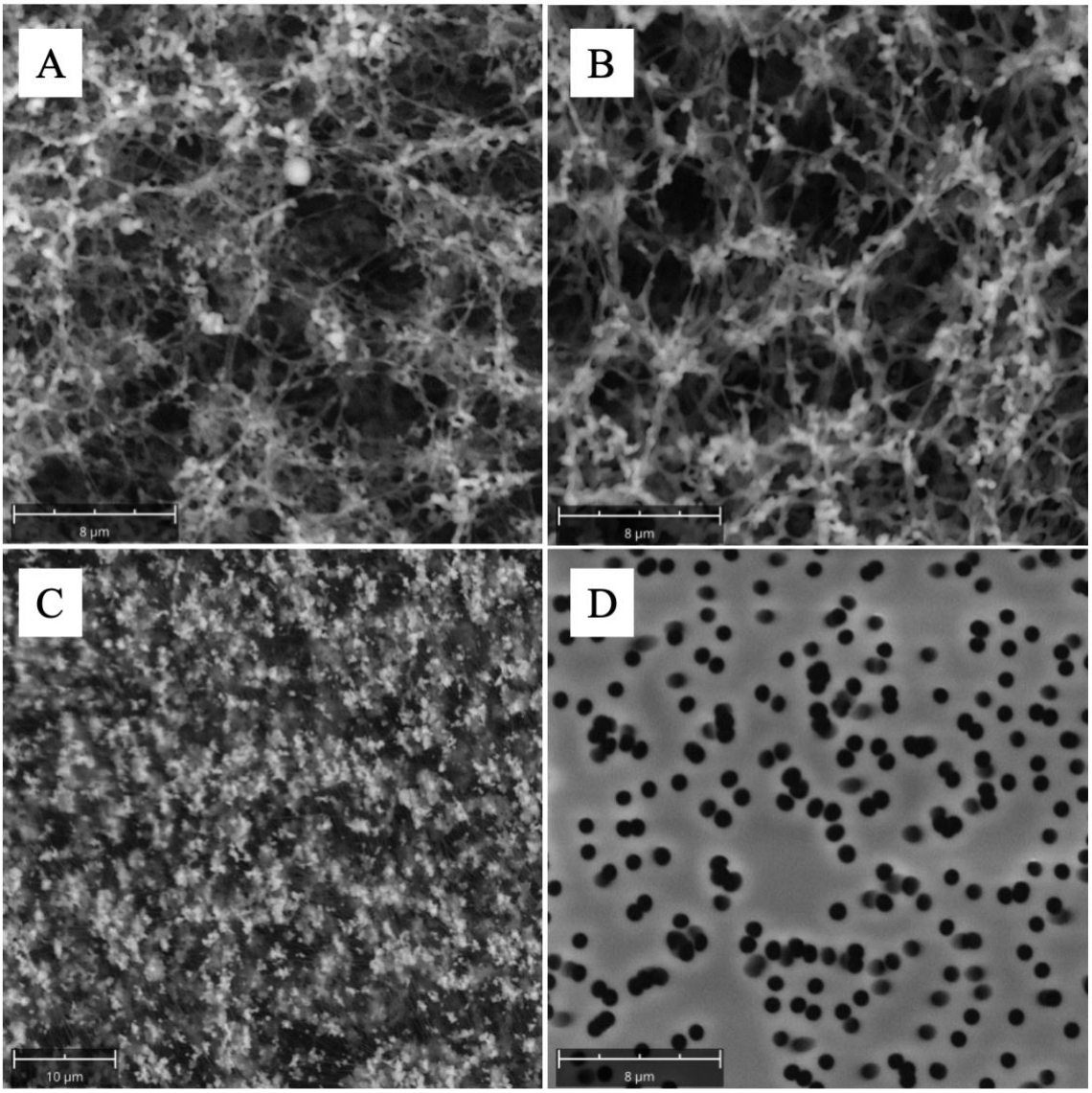

Figure 8: SEM-BSE images of blank (A) MCE 0.45µm, (B) MCE 0.8µm, (C) PTFE 1.0µm, and (D) PC 0.8µm filters.

4.2 Field-exposed filter analysis (Kilauea Volcano, Hawai'i)

Data collection from the 36th eruptive episode of Kilauea resulted in 16 filters, four of each material (MCE 0.45µm, MCE 0.8µm, PC 0.8µm, PTFE 1.0µm). Two MCE 0.45µm, one sampled open-faced and the other with a pump, were used for SEM-BSE imaging. Each showed small, rounded PM ranging from roughly 0.5µm to over 2µm and from semi-rounded to near

perfectly spherical. The PM typically displayed as brighter compared to the surrounding filter when imaged with the SEM-BSE, seen in Figure 9. A few larger particles ranging from 8µm to over 30µm were noted but were infrequent. These stood out against the fine mesh of the filter and small size of the rounded particles. The larger particles had no uniformity in terms of shape, size, texture, or brightness (Figure 10). Smaller particles were harder to distinguish amid the brightness of the filter. The MCE material commonly experienced electron beam alteration that began the instant the electron beam encountered the filter (Figure 11). The alteration resulted in square patches that darkened with the duration of contact. Smaller particles, typically less than 3µm, were usually not affected. Larger particles, greater than around 5µm, were more commonly affected. The filter alteration is noted by the incremental disappearance of sections of the particle, radiating outward from a starting location. In preliminary testing it was seen that larger pieces that had not adequately adhered to the filter would get pushed/moved by the electron beam and no longer be visible.

Although the blank filter displayed false bright spots when at high magnification based on observation, it does appear that the field-exposed MCE filters did collect PM (see the comparison of filters in Figure 9). Although a particle count was not undertaken, SEM-Energy Dispersive X-ray Spectroscopy (SEM-EDS) was conducted on larger PM. Using the SEM-EDS silicates and salts were identified. Larger particles are seen in Figure 10.

The geochemical results, seen in Table 1, indicate that the MCE 0.8µm obtained the most PM (ng/g) with higher levels of Zn, Sr, B, and Ta compared to the other filters. The PTFE, PC, and MCE 0.45µm filters did not appear to have near the quantity of PM as the MCE 0.8µm. However, a few relevant signatures were present such as higher Al and Fe for one PTFE filter,

higher Cu on another PTFE filter, and one PC filter with higher Mg. These signatures were not consistent across the other filters of the same material.

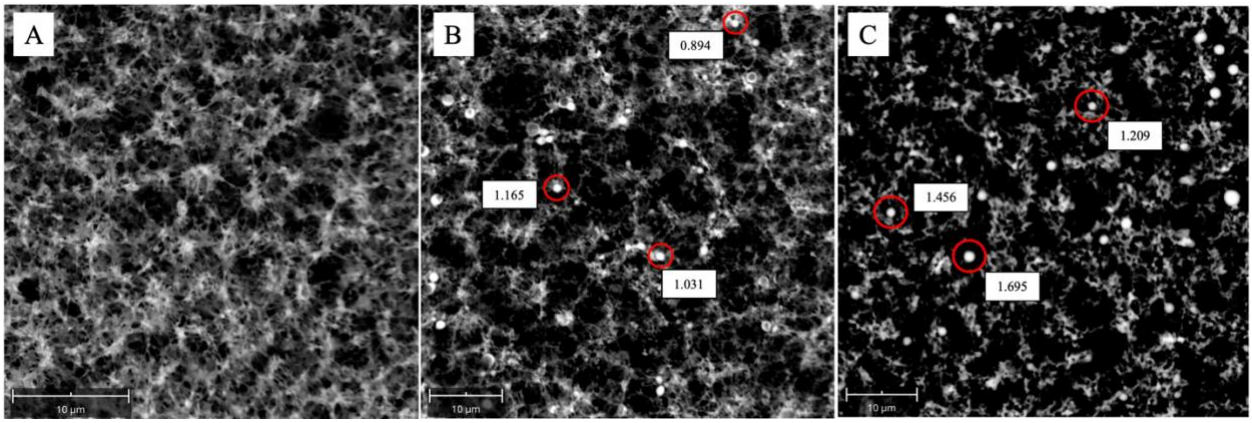

Figure 9: SEM-BSE images of MCE 0.45 filters at 10µm scale. (A) blank. (B) sampled in Kilauea with a pump seen in Figure 4B. (C) sampled in Kilauea with open-faced seen in Figure 5A. PM measured in µm and circled in red for reference.

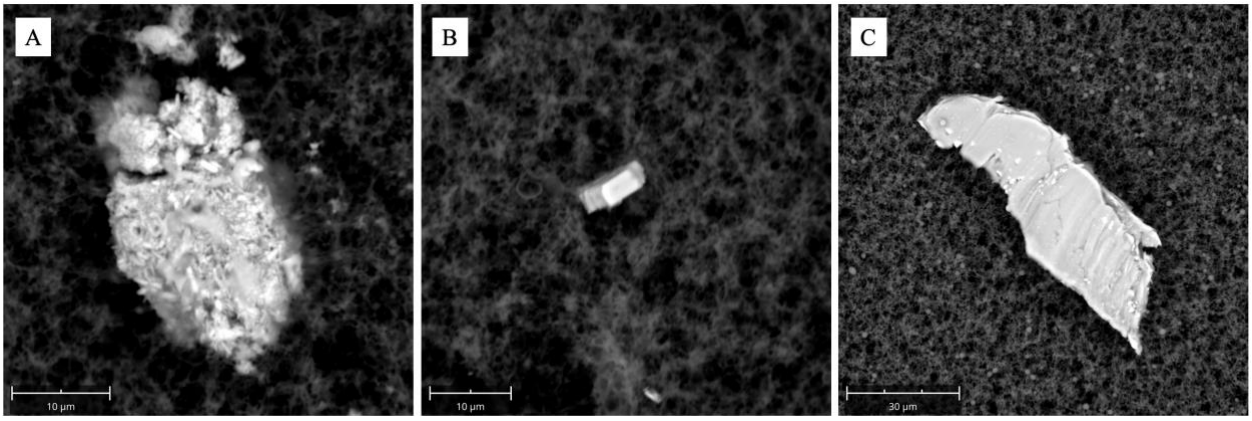

Figure 10: SEM-BSE image, MCE 0.45µm filter (sample taken open-faced at Kilauea Volcano, November 2025) SEM-BSE imaging of larger particles for reference. (A) 10µm scale. (B) 10µm scale. (C) 30µm scale.

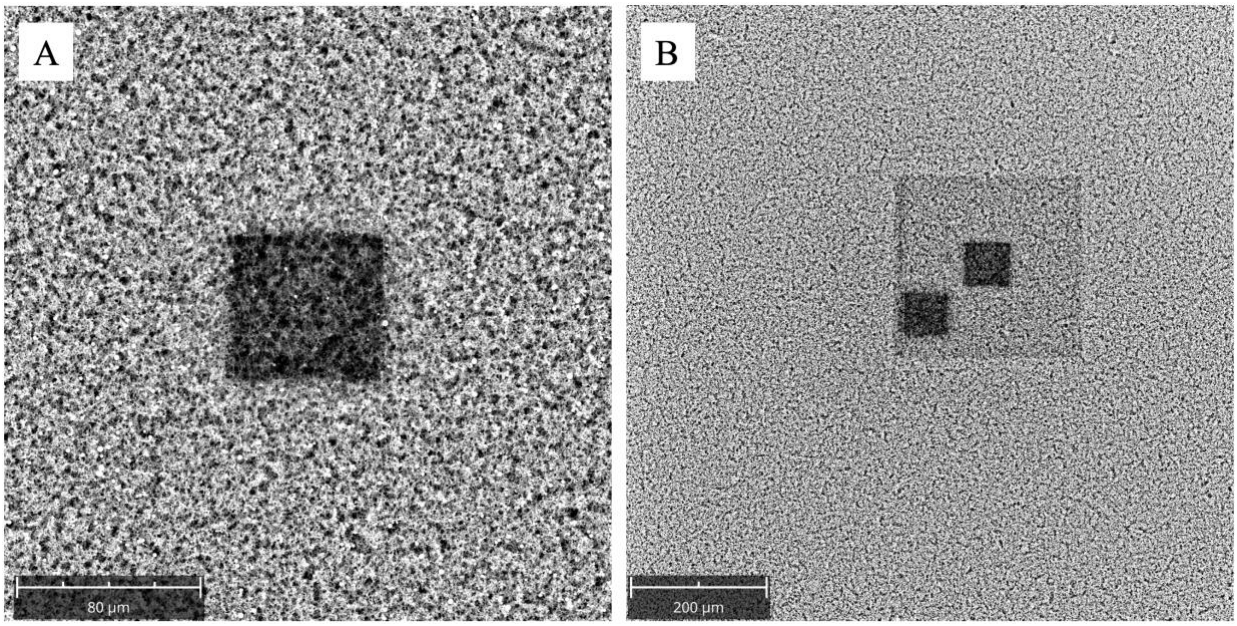

Figure 11: SEM-BSE image, MCE 0.45µm filter (sample taken open-faced at Kilauea Volcano, November 2025) undergoing electron beam caused alteration. (A) 80µm scale (B) 200µm scale.

Table 1: Geochemical analysis summary for the Kilauea filters.

Sample	Re (ng/g)	Pd (ng/g)	Pt (ng/g)	Ru (ng/g)	Ir (ng/g)	Mg (ng/g)	Al (ng/g)	Ca (ng/g)	Fe (ng/g)	Ni (ng/g)	Cu (ng/g)	Zn (ng/g)	Sr (ng/g)	Ba (ng/g)	Ta (ng/g)
HJ1O-PC	0.007		0.251	0.011	0.002	2.05	3.02	15.87	7.28	0.14	0.08	0.85	0.06	0.01	0.09
HJ1P-PC	0.005		0.102	0.007		2.18	4.05	17.81	3.75	0.14	0.08	0.85	0.04	0.01	0.1
HJ1O-PTFE	0.005		0.104	0.005		4.31	1.81	13.06	3.13	0.26	0.92	0.97	0.02	0.06	0.12
HJ1P-PTFE	0.005	0.006	0.086	0.004	0.002	2.41	2.15	8.74	2.9	0.16	0.11	0.48	0.02	0.07	0.13
HJ1O-MCE0.8	0.004	0.086	0.275	0	0.015	5.3	3.59	36.08	7.09	0.21	0.08	0.68	0.31	0.35	1.64
HJ1P-MCE0.8	0.006		0.094	0.007	0.001	5.93	4.52	38.43	6.8	0.22	0.08	0.35	0.34	0.38	1.81
HJ2O-PC	0.005	0.007	0.024	0.005		10.43	3.87	17.2	6	0.14	0.14	0.55	0.06	0.03	0.12
HJ2P-PC	0.005	0.009	0.024	0.002	0.001	3.03	3.4	13.61	2.86	0.14	0.08	0.38	0.03	0.02	0.11
HJ2O-PTFE	0.005		0.025	0.006	0.003	4.38	6.82	7.37	13.09	0.24	0.14	0.67	0.01	0.11	0.1
HJ2P-PTFE	0.003	0.005	0.012	0.003		1.83	4.43	5.52	3.47	0.2	0.08		0.01	0.11	0.11
HJ2O-MCE0.8	0.003	0.027	0.03	0.008	0.002	8.55	8.6	52.04	12.81	0.24	0.19	1.93	0.4	0.43	1.75
HJ2P-MCE0.8	0.004	0.337	0.091	0.309	0.118	13.12	4.39	44.11	8.1	0.28	0.1	1.26	0.35	0.39	1.69
HJ2O-MCE0.45	0.002	0.008	0.091		0.001	8.62	6.02	40.08	9.75	0.15	0.23	0.78	0.2	0.27	0.19
HJ2P-MCE0.45	0.002	0.012	0.074	0.004	0.004	8.48	4.88	40.48	6.76	0.28	0.28	0.6	0.19	0.27	0.18
Blank	0.003	0.022	0.012	0.007		9.15	2.35	41.47	3	0.05	0.01	0.48	0.03	0.01	0.43
Blank	0.004	0.301	0.008	0.007	0.014	1.93	3.53	7	2.24	0.04			0.01		0.12

4.3 Lab "bench" test comparison of MCE and PTFE filters

A lab-based "bench" test was done to compare MCE and PTFE filters. This test involved artificially contaminating MCE 0.8µm and PTFE 1.0µm filters with sieved tephra to simulate sampling with a pump. Filters were qualitatively analyzed. A key difference noted is that the MCE 0.8µm filter had a small, visible, rounded, dark discoloration at the center of the filter with fan-shaped area of larger particle collection descending from the center (Figure 12B). Outside of this fan-shaped area particles were present, though observed to be less concentrated. Larger particles were additionally visible at the bottom of the filter canister, not adhering on the filter. In comparison, the PTFE 1.0µm filter had a small concentration of particles, mostly toward the bottom of the filter, and no visible discoloration at the center or anywhere else on the filter (Figure 12D).

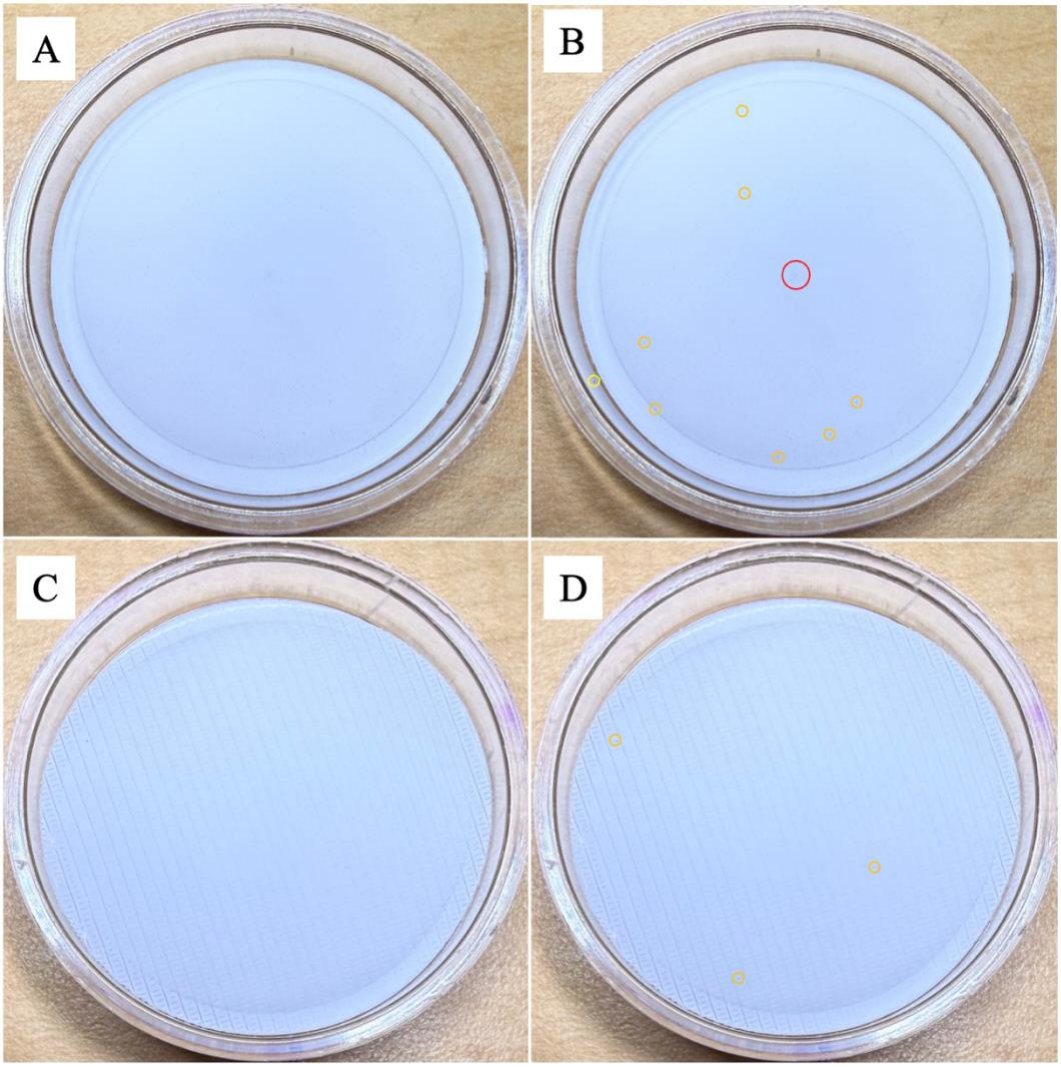

Figure 12: Artificially contaminated filters. (A) and (B) MCE 0.8µm filter, (B) annotated. (C) and (D) PTFE 0.1µm, (D) annotated. Red circle denoting central collection, orange circles a portion of the total particulates on filter, yellow circle particulates not on filter.

5. DISCUSSION

5.1 SEM filter comparison

When comparing the ground sampled open-face and pump-sampled MCE 0.45µm filters from Kilauea on the SEM there is not a significant observational difference noticed. This is likely because the ground sampling did not have any forced air flow as a UAV might. However, for the purposes of quantifying PM the use of a pump is suggested to allow for a known air flow rate. Interestingly, it was found that on both MCE 0.45µm filters there was a section of the filter with less particles than the other areas. This may be a result of particle weight or airflow and is an interesting aspect to pursue in further research. Future sampling would benefit from labeling the top, bottom, and sides of the filter as it is oriented during sampling.

Blank filter SEM-BSE images, seen in Table 2, provided information about the quality of the image that can be taken, effects of the electron beam on the filter material, and visibility of the pore sizes of each filter (seen in Table 2). The three types of filter materials were all unique and required specific imaging techniques for best viewing. The PTFE filter was simply too difficult to image, especially at a high magnification. The PC filter did not appear to have an adequate adhering surface, its pores seemed dispersed at random, and the filter looked to be 2-dimensional compared to the intertwined 3-dimensional depth of the MCE filter. When the pore size was measured, each were roughly 0.8µm, highlighting the uniformity. Importantly, the MCE filters did experience alteration caused by the electron beam and displayed bright spots that could be mis-identified as small PM. Thus, the filter material and subsequent alteration influenced visibility of the particles when analyzing. Imaging the MCE filters with different pore sizes, 0.8µm and 0.45µm, showed that there are noticeably larger gaps between the fibers of the filter

in the 0.8µm pore sized filter. Both displayed intertwined fibers that accentuated the depth of filter.

Examining the filter via SEM does pose limitations, as mentioned. Nevertheless, the visual comparison of the blank filters in combination with filter type descriptions (Table 2) is a useful tool to when considering research approaches and analytical methods that work best for specific areas of study.

5.2 Geochemical comparison of the filters

The geochemical analysis is preliminary and limited because of the small concentration of PM found on the filters. As a reminder, these filters were exposed 7 km from an active vent, on the ground; in future work the hope is to fly the UAV into the plume much closer to an active vent. Sampling limitations notwithstanding, overall, the MCE 0.8µm filter appears to be the most successful at capturing PM. Limitations of equipment used further highlights the need to sample closer to and/or within the plume. When conducting such analysis of the filters, a more focused approach for testing what is present may be beneficial and more capable for the equipment considering the small amount thought to be on the filter. Additionally, understanding how the filters reacted to the HF was useful in understanding what may or may not have been present in the leachate that was examined as each filter type had a unique reaction to the HF. The MCE dissolved rapidly and fully, while the PTFE remained fully intact and appeared unchanged. The PC was somewhere in between; it did not completely dissolve but was visibly altered. Initially the PC filter was white and flexible, however after the being exposed to HF it became tinted green and more brittle. Therefore, the leachate of the MCE contained the entire filter,

while the PTFE leachate was likely just what was on the filter. The PC filter possibly had some contribution in addition to what collected on to the filter.

5.3 Comprehensive comparison of filter types

Considering the geochemical and SEM data comparison of the filters, a comparison of how the PM will adhere to the filter material is essential in choosing sampling material. Given that the PTFE appeared to be unaffected by HF, SEM-BSE imaging to examine the pore size and filter texture proved to be difficult due to the nature of PTFE, this filter type is likely not adequate at catching and maintain possession of PM. The PC filter was altered by HF in the lab preparation process for analysis, and the SEM imaging displayed the filter as flat and with not much texture. Lastly, despite that the MCE fully dissolved when in contact with HF, the SEM-BSE imaging clearly showed the depth, texture, and fibrous material of the filter. In addition, given that the Hawai'i filters clearly displayed PM, seen in Figures 2A and 2B, the MCE is suggested to be the most durable in terms of PM adhering to the filter and remaining there for analysis, however the precise reasoning for this is still unknown. During the lab-based filter material comparison test it was observed that significantly more material adhered to the MCE 0.8µm filter as compared to the PTFE 1.0µm filter. Both experienced visible gravitational settling and larger particles not adhering to the filter. As a result of this assessment, in combination with the SEM and geochemical data, it was determined that an MCE type filter is likely the most capable at catching and retaining PM. A comprehensive comparison of filter types is seen in Table 2 with SEM-BSE imaging providing qualitative visual data.

Table 2: Summary of the three filter materials and four pore sizes tested. Material, Pore size, Reaction with acid, and Blank SEM-BSE images for MCE, PTFE, and PC depicted.

	MCE		**PTFE**	**PC**
Material	Mixed Cellulose Ester		Polytetrafluoroethylene	Polycarbonate
Pore size	0.45µm	0.8µm	1.0µm	0.8µm
Reaction with acid	Fully dissolved	Fully dissolved	Appeared unaltered	Partially altered
Blank SEM-BSE images	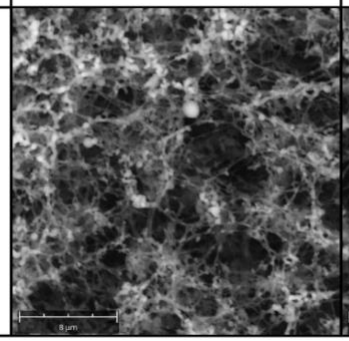	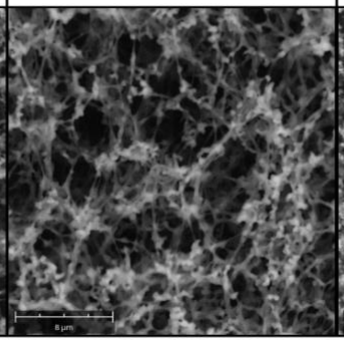	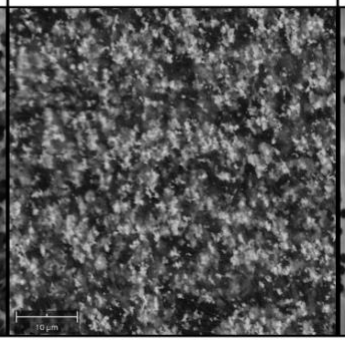	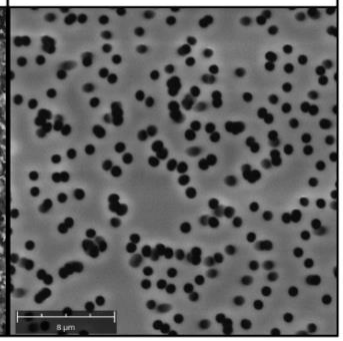

5.4 Implications for future work

Observational and geochemical data show that a 7 km sampling distance will result in PM on filters, however the concentrations are too low for the equipment to analyze the concentrations properly. A logical conclusion is that using a UAV to fly directly within the plume would be far more effective. A sampling duration of 10-20 minutes is likely a sufficient sampling time directly downwind of and within the plume. For ground-based sampling, however, a longer sampling time may yield better results, especially if at a considerable distance from the vent. Regarding the use of a pump, based on SEM data it does not appear to be vital in PM collection amount in either a positive or negative way. However, a pump with a known air flow allows for particle concentration to be quantified to a common metric, L/min, if an estimate of the amount of PM on a filter were obtained. Though the MCE and PTFE comparison "bench" test showed that the filters are different, further analysis would be useful in determining variables such as filter capacity, level of PM retention, and effect on air flow. Based on results from this work, MCE filter material is recommended to be used in future sampling as it has proven to be more adherent than the PTFE filter material.

When comparing the findings of this work to the existing literature, for example research indicating high amounts of Iridium from Kilauea volcano (Olmez et al., 1986), this work poses to establish a defined method for the sole collection of PM rather than combining it with gas sampling as in most studies. Limitations of the data provided are regarding the amount of real field data collected. Iceland is the ideal and preferred sampling location, however within the time constraint of this thesis there was no active eruptive activity. Therefore, Hawai'i proved to be a less ideal alternative for sampling and only ground sampling was able to be conducted. When

Iceland erupts, proximal aerial sampling will be conducted and allow for a more comprehensive collection of data to be presented.

6. CONCLUSION

Effusive basaltic eruptions allow for exceptional sampling opportunities for PM that can provide insight into topics such as magma source, crustal contamination, magma generation, degree of fractionation, and PM distribution. The current literature discussing volcanism plume sampling is lacking in detail regarding techniques and PM focused collection. This work provides constraints and insight into best sampling practices, including materials, sampling duration, and proximity to vent while providing a launching point for further research into effective PM sampling. SEM-BSE imaging and geochemical analysis of filters conducted was successful, specifically looking for PM rather than gas. The Kilauea 36th eruptive episode allowed for a unique opportunity to test different variables in relation to volcanic PM sampling. A preferred location, however, is one that permits both proximal ground and aerial sampling for regular basaltic volcanism, such as Iceland. The variables tested include filter type, pore size, pump, and open- or closed-faced filter. Both quantitative and qualitative assessments of the data was done to compare aerial and ground-based sampling in addition to the sampling variables mentioned. Based on the data presented, aerial sampling in the plume is suggested to be the most ideal as this would be the closest sampling that could be safely done. Ground sampling techniques may prove to be more effective if conducted closer to the vent and sample duration were to be longer. Pumped filtration provides a unit of measure, in L/min, to quantify geochemical data and particle counting. MCE filters are interpreted to be the most adherent and thus most effective at catching and retaining PM. Although electron beam alteration is likely to occur when conducting SEM-BSE imaging, the other filter types were not any more suitable, and in the case of PTFE the conditions for imaging were worse.

In terms of geochemical analysis, the presented data displays the capabilities that should be considered when choosing a filter type and based off the samples collected the MCE filter type is recommended. Even though the MCE fully dissolves during analysis preparation, it is likely to have more particles adhering to it compared to the other filter types. In future sampling, being closer to the vent will theoretically yield a higher concentration of PM and therefore the equipment used for geochemical analysis will be more capable. This would provide an opportunity to compare the sampling variables under more intense conditions while also assessing the capabilities of the aerial sampling apparatus. Alternate analysis tools may prove useful in future studies.

REFERENCES

Aiuppa, A., Bellomo, S., D'Alessandro, W., Federico, C., Ferm, M., & Valenza, M. (2004). Volcanic plume monitoring at Mount Etna by diffusive (passive) sampling. *Journal of Geophysical Research: Atmospheres*, *109*(D21). https://doi.org/10.1029/2003JD004481

Aiuppa, A., Federico, C., Paonita, A., Pecoraino, G., & Valenza, M. (2002). S, Cl and F degassing as an indicator of volcanic dynamics: The 2001 eruption of Mount Etna. *Geophysical Research Letters*, *29*(11), 54-1-54–4. https://doi.org/10.1029/2002GL015032

Allen, A. G., Baxter, P. J., & Ottley, C. J. (2000). Gas and particle emissions from Soufrière Hills Volcano, Montserrat, West Indies: Characterization and health hazard assessment. *Bulletin of Volcanology*, *62*(1), 8–19. https://doi.org/10.1007/s004450050287

Aurell, J., & Gullett, B. K. (2024). Effects of UAS Rotor Wash on Air Quality Measurements. *Drones*, *8*(3), 73. https://doi.org/10.3390/drones8030073

Crocket, J. H., & Paul, D. K. (2004). Platinum-group elements in Deccan mafic rocks: A comparison of suites differentiated by Ir content. *Chemical Geology, Highly Siderophile Element Behavior in High Temperature Processes*, *208*(1), 273–291. https://doi.org/10.1016/j.chemgeo.2004.04.017

Crowe, B. M., Finnegan, D. L., Zoller, W. H., & Boynton, W. V. (1987). Trace element geochemistry of volcanic gases and particles from 1983–1984 eruptive episodes of Kilauea Volcano. *Journal of Geophysical Research: Solid Earth*, *92*(B13), 13708–13714. https://doi.org/10.1029/JB092iB13p13708

Day, J. M. D., Waters, C. L., Schaefer, B. F., Walker, R. J., & Turner, S. (2016). Use of Hydrofluoric Acid Desilicification in the Determination of Highly Siderophile Element Abundances and Re-Pt-Os Isotope Systematics in Mafic-Ultramafic Rocks. *Geostandards and Geoanalytical Research*, *40*(1), 49–65. https://doi.org/10.1111/j.1751-908X.2015.00367.x

Finnegan, D. L., Kotra, J. P., Hermann, D. M., & Zoller, W. H. (1989). The use of7LiOH-impregnated filters for the collection of acidic gases and analysis by instrumental neutron activation analysis. *Bulletin of Volcanology*, *51*(2), 83–87. https://doi.org/10.1007/BF01081977

Hawaiian Volcano Observatory (2025). November 25, 2025—Kīlauea summit eruption reference map. *U.S. Geological Survey.* https://www.usgs.gov/media/images/november-25-2025-kilauea-summit-eruption-reference-map

Hedworth, H. A., Sayahi, T., Kelly, K. E., & Saad, T. (2021). The effectiveness of drones in measuring particulate matter. *Journal of Aerosol Science*, *152*, 105702. https://doi.org/10.1016/j.jaerosci.2020.105702

Hinkley, T. K. (1991). Distribution of metals between particulate and gaseous forms in a volcanic plume. *Bulletin of Volcanology*, *53*(5), 395–400. https://doi.org/10.1007/BF00280229

Ilyinskaya, E., Mason, E., Wieser, P. E., Holland, L., Liu, E. J., Mather, T. A., Edmonds, M., Whitty, R. C. W., Elias, T., Nadeau, P. A., Schneider, D., McQuaid, J. B., Allen, S. E., Harvey, J., Oppenheimer, C., Kern, C., & Damby, D. (2021). Rapid metal pollutant deposition from the volcanic plume of Kīlauea, Hawai'i. *Communications Earth & Environment*, *2*(1), 1–15. https://doi.org/10.1038/s43247-021-00146-2

Ilyinskaya, E., Schmidt, A., Mather, T. A., Pope, F. D., Witham, C., Baxter, P., Jóhannsson, T., Pfeffer, M., Barsotti, S., Singh, A., Sanderson, P., Bergsson, B., McCormick Kilbride, B., Donovan, A., Peters, N., Oppenheimer, C., & Edmonds, M. (2017). Understanding the environmental impacts of large fissure eruptions: Aerosol and gas emissions from the 2014–2015 Holuhraun eruption (Iceland). *Earth and Planetary Science Letters*, *472*, 309–322. https://doi.org/10.1016/j.epsl.2017.05.025

Kim, W. Y., Lee, S. G., Lee, H., & Ahn, K.-H. (2025). Investigation of Vertical Profiles of Particulate Matter and Meteorological Variables up to 2.5 km in Altitude Using a Drone-Based Monitoring System. *Atmosphere*, *16*(1), 93. https://doi.org/10.3390/atmos16010093

Mandon, C. L., Christenson, B. W., Schipper, C. I., Seward, T. M., & Garaebiti, E. (2019). Metal transport in volcanic plumes: A case study at White Island and Yasur volcanoes. *Journal of Volcanology and Geothermal Research*, *369*, 155–171. https://doi.org/10.1016/j.jvolgeores.2018.11.024

Martin, R. S., Mather, T. A., Pyle, D. M., Power, M., Allen, A. G., Aiuppa, A., Horwell, C. J., & Ward, E. P. W. (2008). Composition-resolved size distributions of volcanic aerosols in the Mt. Etna plumes. *Journal of Geophysical Research: Atmospheres*, *113*(D17). https://doi.org/10.1029/2007JD009648

Mason, E., Edmonds, M., & McConnell, J. R. (2022). Volatile trace metals deposited in ice as soluble volcanic aerosols during the 17.7.ka eruptions of Mt Takahe, West Antarctic Rift. *Frontiers in Earth Science*, *10*. https://doi.org/10.3389/feart.2022.1002366

Mason, E., Wieser, P. E., Liu, E. J., Edmonds, M., Ilyinskaya, E., Whitty, R. C. W., Mather, T. A., Elias, T., Nadeau, P. A., Wilkes, T. C., McGonigle, A. J. S., Pering, T. D., Mims, F. M., Kern, C., Schneider, D. J., & Oppenheimer, C. (2021). Volatile metal emissions from volcanic degassing and lava–seawater interactions at Kīlauea Volcano, Hawai'i. *Communications Earth & Environment*, *2*(1), 1–16. https://doi.org/10.1038/s43247-021-00145-3

Mather, T. A., Allen, A. G., Oppenheimer, C., Pyle, D. M., & McGonigle, A. J. S. (2003). Size-Resolved Characterisation of Soluble Ions in the Particles in the Tropospheric Plume of Masaya Volcano, Nicaragua: Origins and Plume Processing. *Journal of Atmospheric Chemistry*, *46*(3), 207–237. https://doi.org/10.1023/A:1026327502060

Mather, T. A., Pyle, D. M., & Heaton, T. H. E. (2008). Investigation of the use of filter packs to measure the sulphur isotopic composition of volcanic sulphur dioxide and the sulphur and oxygen isotopic composition of volcanic sulphate aerosol. *Atmospheric Environment*, *42*(19), 4611–4618. https://doi.org/10.1016/j.atmosenv.2008.01.052

Mather, T. A., Witt, M. L. I., Pyle, D. M., Quayle, B. M., Aiuppa, A., Bagnato, E., Martin, R. S., Sims, K. W. W., Edmonds, M., Sutton, A. J., & Ilyinskaya, E. (2012). Halogens and trace metal emissions from the ongoing 2008 summit eruption of Kīlauea volcano, Hawai`i. *Geochimica et Cosmochimica Acta*, *83*, 292–323. https://doi.org/10.1016/j.gca.2011.11.029

Menard, G., Moune, S., Vlastélic, I., Aguilera, F., Valade, S., Bontemps, M., & González, R. (2014). Gas and aerosol emissions from Lascar volcano (Northern Chile): Insights into the origin of gases and their links with the volcanic activity. *Journal of Volcanology and Geothermal Research*, *287*, 51–67. https://doi.org/10.1016/j.jvolgeores.2014.09.004

Messling, N., Willbold, M., Kallas, L., Elliott, T., Fitton, J. G., Müller, T., & Geist, D. (2025). Ru and W isotope systematics in ocean island basalts reveals core leakage. *Nature*, 1–5. https://doi.org/10.1038/s41586-025-09003-0

Moune, S., Gauthier, P.-J., & Delmelle, P. (2010). Trace elements in the particulate phase of the plume of Masaya Volcano, Nicaragua. *Journal of Volcanology and Geothermal Research*, *193*(3), 232–244. https://doi.org/10.1016/j.jvolgeores.2010.04.004

Naughton, J. J., Lewis, V., Thomas, D., & Finlayson, J. B. (1975). Fume compositions found at various stages of activity at Kilauea Volcano, Hawaii. *Journal of Geophysical Research (1896-1977)*, *80*(21), 2963–2966. https://doi.org/10.1029/JC080i021p02963

Olmez, I., Finnegan, D. L., & Zoller, W. H. (1986). Iridium emissions from Kilauea Volcano. *Journal of Geophysical Research: Solid Earth*, *91*(B1), 653–663. https://doi.org/10.1029/JB091iB01p00653

Pfeffer, M. A., Doukas, M. P., Werner, C. A., & Evans, W. C. (2013). Airborne filter pack measurements of S and Cl in the plume of Redoubt Volcano, Alaska February–May 2009. *Journal of Volcanology and Geothermal Research, The 2009 Eruption of Redoubt Volcano, Alaska*, *259*, 285–289. https://doi.org/10.1016/j.jvolgeores.2012.04.011

Shimura, T., Inoue, M., Tsujimoto, H., Sasaki, K., & Iguchi, M. (2018). *Estimation of Wind Vector Profile Using a Hexarotor Unmanned Aerial Vehicle and Its Application to Meteorological Observation up to 1000 m above Surface*. https://doi.org/10.1175/JTECH-D-17-0186.1

Shinohara, H. (2005). A new technique to estimate volcanic gas composition: Plume measurements with a portable multi-sensor system. *Journal of Volcanology and Geothermal Research*, *143*(4), 319–333. https://doi.org/10.1016/j.jvolgeores.2004.12.004

Shinohara, H., & Witter, J. B. (2005). Volcanic gases emitted during mild Strombolian activity of Villarrica volcano, Chile. *Geophysical Research Letters*, *32*(20). https://doi.org/10.1029/2005GL024131

Stefánsson, A., Stefánsdóttir, G., Keller, N. S., Barsotti, S., Sigurdsson, Á., Thorláksdóttir, S. B., Pfeffer, M. A., Eiríksdóttir, E. S., Jónasdóttir, E. B., von Löwis, S., & Gíslason, S. R. (2017). Major impact of volcanic gases on the chemical composition of precipitation in Iceland during the 2014–2015 Holuhraun eruption. *Journal of Geophysical Research: Atmospheres*, *122*(3), 1971–1982. https://doi.org/10.1002/2015JD024093

Tipayarom, D., Santisophonkul, T., & Tipayarom, A. (2024). Development of Low-Cost Particulate Matter Monitoring Drone System. *Advances in Science and Technology*, *150*, 47–53. https://doi.org/10.4028/p-Wwl5JW

Tran, A. T. P. (2019). *Drone in Particulate Matter Measurement* [fi=AMK-opinnäytetyö|sv=YH-examensarbete|en=Bachelor's thesis|]. http://www.theseus.fi/handle/10024/226764

Wainman, L. (2024). Using drones to sample volcanic plumes. *Nature Reviews Earth & Environment*, *5*(7), 484–484. https://doi.org/10.1038/s43017-024-00570-w

Wittmer, J., Bobrowski, N., Liotta, M., Giuffrida, G., Calabrese, S., & Platt, U. (2014). Active alkaline traps to determine acidic-gas ratios in volcanic plumes: Sampling techniques and analytical methods. *Geochemistry, Geophysics, Geosystems*, *15*(7), 2797–2820. https://doi.org/10.1002/2013GC005133

Zoller, W. H., Parrington, J. R., & Phelan Kotra, J. M. (1983). Iridium Enrichment in Airborne Particles from Kilauea Volcano: January 1983. *Science*, *222*(4628), 1118–1121. https://doi.org/10.1126/science.222.4628.1118